

# Preparation of $\alpha$ -Fe<sub>2</sub>O<sub>3</sub> nanostructures via simple ultrasound-assisted method

J. HASANZADEH<sup>\*</sup>, Y. AZIZIAN-KALANDARAGH<sup>a</sup>, A. KHODAYARI<sup>b</sup>

*Department of Physics, Faculty of Science, Islamic Azad University, Takestan Branch, Takestan, Iran*

*<sup>a</sup>Department of Physics, University of Mohaghegh Ardabili, P.O. Box 179, Ardabil, Iran*

*<sup>b</sup>Department of Chemistry, University of Mohaghegh Ardabili, P.O. Box 179, Ardabil, Iran*

This study involves the preparation of  $\alpha$ -Fe<sub>2</sub>O<sub>3</sub> (hematite) nanoparticles via simple and facile ultrasound-assisted method from aqueous solution of FeSO<sub>4</sub>·7H<sub>2</sub>O and NaOH in the presence of 3-MPA as a capping agent. X-ray diffraction analysis exhibits that the as-prepared product are in the phase of FeO(OH) and excellently crystallized  $\alpha$ -Fe<sub>2</sub>O<sub>3</sub> nanostructures have been formed after thermal annealing at 450°C. Scanning electron microscope (SEM) images reveal that the product consisting of rod-like nanocrystallites of about 40nm width and 300nm length, which aggregated in the form of polydispersive clusters. The FT-IR absorption spectroscopy of the as-prepared nanostructures and annealed nanopowders were studied.

(Received April 9, 2012; accepted June 6, 2012)

*Keywords:* SEM,  $\alpha$ -Fe<sub>2</sub>O<sub>3</sub> nanoparticles, XRD, FT-IR

## 1. Introduction

Metal oxide nanomaterials exhibiting interesting optical and electrical properties that can be grown efficiently as powder nanostructures are used extensively for variety of applications in catalysis, sensors, environmental remediation and optoelectronic devices [1-7]. Among different metal oxides, iron oxide nanoparticles received great attention because of its potential applications in technological applications such as recording media, biosensors, biomedicine, passive and active targeting, ferrofluids, optical power limiting agent and biogeochemical processes [8-16].

Controlled preparation of metal oxide nanoparticles is essential for successful application, and several synthetic methods have been developed for synthesizing metal oxide nanoparticles over the past several decades. There are also several important for preparation of metal oxide nanoparticles, such as: synthesis of pure nanostructures, shape and size control, maintaining a narrow size distribution, control of degree of crystallinity and structure. Recently, ultrasonic-assisted method has been the topic of intense investigation in the synthesis of nanostructures due to low-cost, simple and effective route. Due to special sonochemical reaction effect, the ultrasound-assisted preparation method has advantages such as a rapid crystallization, controllable morphology and size high purity [17-21].

In this paper, we report preparation and characterization of nanocrystalline  $\alpha$ -Fe<sub>2</sub>O<sub>3</sub> by the ultrasound-assisted method. The nanocrystalline FeO(OH) and  $\alpha$ -Fe<sub>2</sub>O<sub>3</sub> was synthesized by sonication an aqueous solution of FeSO<sub>4</sub>·7H<sub>2</sub>O and NaOH. The as prepared nanoparticles were analyzed by X-ray diffraction (XRD),

scanning electron microscopy (SEM) and Fourier transform infrared (FT-IR) spectroscopy.

## 2. Experimental

### 2.1 Materials and preparation of $\alpha$ -Fe<sub>2</sub>O<sub>3</sub> nanostructures

Ferrous sulfate heptahydrate (FeSO<sub>4</sub>·7H<sub>2</sub>O), ammonium hydroxide (NaOH), 3-MPA (3-mercaptopropionic acid) and absolute ethanol were obtained from Merck and employed without further purification. Double distilled water was used for washing the particles.

In a typical procedure 0.2M solution of Ferrous sulfate was prepared by dissolving 1.39 g FeSO<sub>4</sub>·7H<sub>2</sub>O in 25ml distilled water. The pH of the solution was 4. In a different flask 0.4M aqueous solution of sodium hydroxide was prepared by dissolving 0.4 g NaOH in 25 ml distilled water and the pH amount of the solution was 12. These solutions were mixed together in a rounded bottom flask and 1mmol 3-MPA was added to the mixture and then the product was ultrasonically irradiated for 1 h at room temperature in open air on a laminar flow bench, using Dr. Heilscher high intensity ultrasound processor UP200H Germany (0.3 cm diameter Ti horn, 200 W/cm<sup>2</sup>, 23 kHz). During the sonication of reaction mixture, the temperature increased to about 80°C and the total pH of the solution was 9.

After sonication, the solution was centrifuged (at revolution rate of 4000 rpm) and a plenty of brown precipitates could be observed. The precipitates were washed with double distilled water and absolute ethanol for several times and then were dried at room temperature

for 1 day. To convert the as-prepared FeO(OH) nanostructures into  $\alpha$ -Fe<sub>2</sub>O<sub>3</sub> the as-prepared powders were annealed at 450 C for 2 h in air atmosphere, where the annealing temperature was selected from thermo gravimetric analysis (not shown here).

## 2.2 Characterization Methods

The X-ray powder diffraction (XRD) pattern of product was carried out on Philips X Pert X-ray diffractometer with CuK $\alpha$  radiation ( $\lambda = 0.154$  nm) in the  $2\theta$  range from 15° to 80°. Surface morphology and distribution of particles were performed via LEO 1430VP scanning electron microscope, using an accelerating voltage of 15 kV. The sample used for SEM observations was prepared by transferring the particles, which at first was dispersed in the ethanol to the SEM stage. After allowing the evaporation of ethanol from the stage, the particles on the stage were coated with a thin layer of gold. FT-IR Transmission spectrum of the sample was recorded employing Perkin Elmer RXI spectrometer.

## 3. Results and discussion

### 3.1 XRD results

Fig. 1 (a) and 1(b) represents the X-ray diffraction pattern of the prepared FeO(OH) and  $\alpha$ -Fe<sub>2</sub>O<sub>3</sub> nanostructures, respectively. Diffraction peaks in XRD spectra of the samples corresponding diffraction planes are XRD patterns and clearly indicate the formation of FeO(OH) and  $\alpha$ -Fe<sub>2</sub>O<sub>3</sub> phase with polycrystalline structures [22,23]. Peaks are broadened indicating that the crystals are very small in size. The nanostructures mean size of was approximately estimated by Hall's method [24]:

$$\beta \cos\theta = \frac{\lambda}{D} + 2\epsilon \sin\theta$$

where  $\beta$  is the measured full width at half maximum (FWHM) in radians,  $\theta$  is the Bragg angle of the diffraction peak,  $\lambda$  is the X-ray wavelength,  $D$  is the grain size,  $\epsilon$  is the effective residual strain.

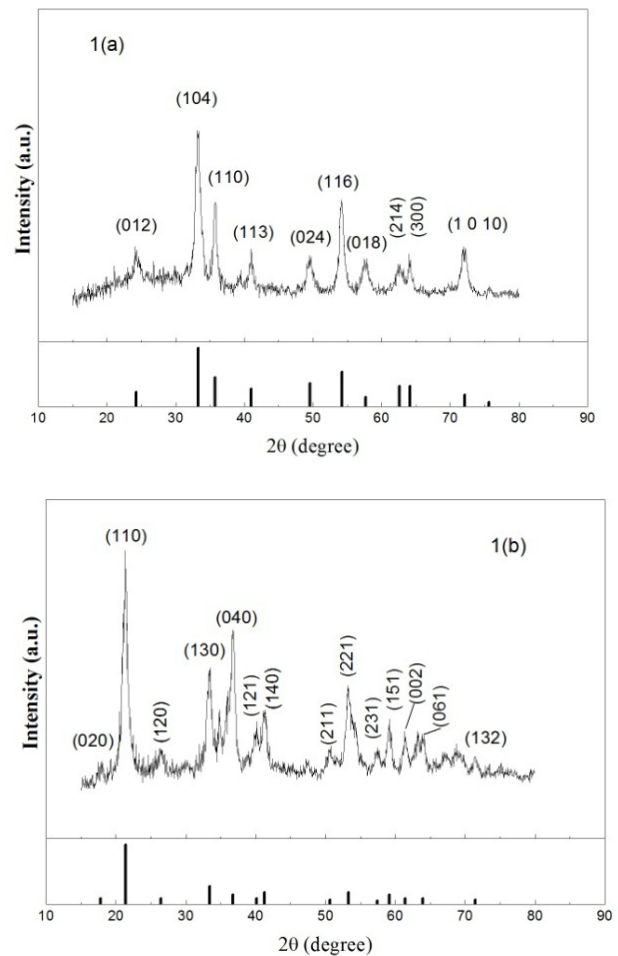


Fig.1 X-ray diffraction spectra for initial sample prepared and dried at room temperature for 1 day indicate the formation of FeO(OH) phase (a) and after thermal annealing at patterns of the prepared samples 1(a) and after thermal annealing at 450 °C the X-ray diffraction spectra clearly indicate the formation of  $\alpha$ -Fe<sub>2</sub>O<sub>3</sub> phase 1(b).

The angle of diffraction ( $2\theta$ ) and peaks miller index of the as-prepared and annealed products are given in Table 1.

Table 1. Diffraction peaks in XRD spectra of the samples and corresponding diffraction planes, at right: the data before annealing and at left, the data after annealing.

2 $\theta$	Diffraction planes	2 $\theta$	Diffraction planes
24.4	(012)	17.8	(020)
33.2	(104)	21.4	(110)
35.8	(110)	26.5	(120)
41	(113)	33.4	(130)
49.6	(024)	36.8	(040)
54.1	(116)	40.1	(121)
57.4	(018)	41.3	(140)
62.4	(214)	50.6	(211)
64.1	(300)	53.3	(221)
72	(1 0 10)	57.4	(231)
		59.1	(151)
		61.4	(002)
		63.9	(061)
		71.5	(132)

Fig. 2(a) and 2(b) represents a typical plot of  $\beta \cos \theta$  vs.  $\sin \theta$  for FeO(OH) and  $\alpha$ -Fe<sub>2</sub>O<sub>3</sub> nanostructures prepared by ultrasound-assisted method respectively.  $\epsilon$  and D can be estimated from the slope of the straight line and the intercept on  $\beta \cos \theta$  axis respectively.

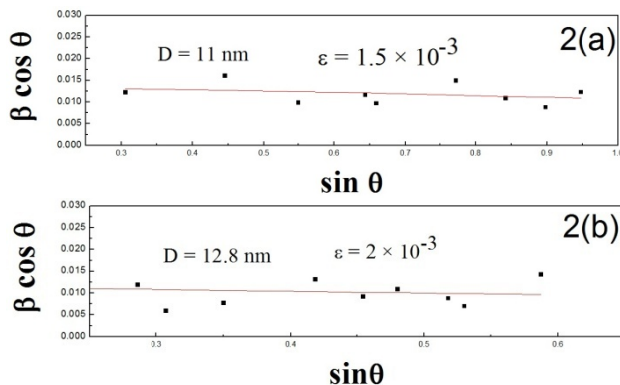


Fig. 2(a). plot of  $\beta \cos \theta$  vs.  $\sin \theta$  for FeO(OH) and 2(b) for  $\alpha$ -Fe<sub>2</sub>O<sub>3</sub> nanostructures prepared by ultrasound-assisted method.

### 3.2 SEM Images

The SEM images of the as-prepared FeO(OH) nanostructures are shown in Fig. 3(a) and (b) at different magnifications. It is clear that as-prepared nanostructures are in rod-type form with polydispersive size distribution. The SEM image of  $\alpha$ -Fe<sub>2</sub>O<sub>3</sub> nanostructures are shown in Fig. 4(a) and (b). As can be seen from Fig. 4 (a) and (b) that the nanostructures have rod-like shape and the length of the maximum number of particles are between 100 to 300nm and width of the particles are about 20 nm to 60nm, approximately.

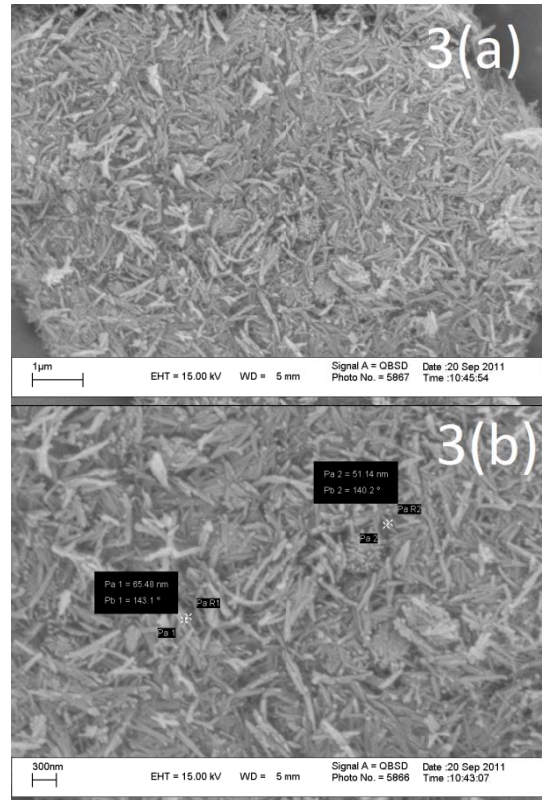


Fig. 3(a) and (b). SEM images of FeO(OH) nanostructures prepared by ultrasound-assisted method at different magnifications.

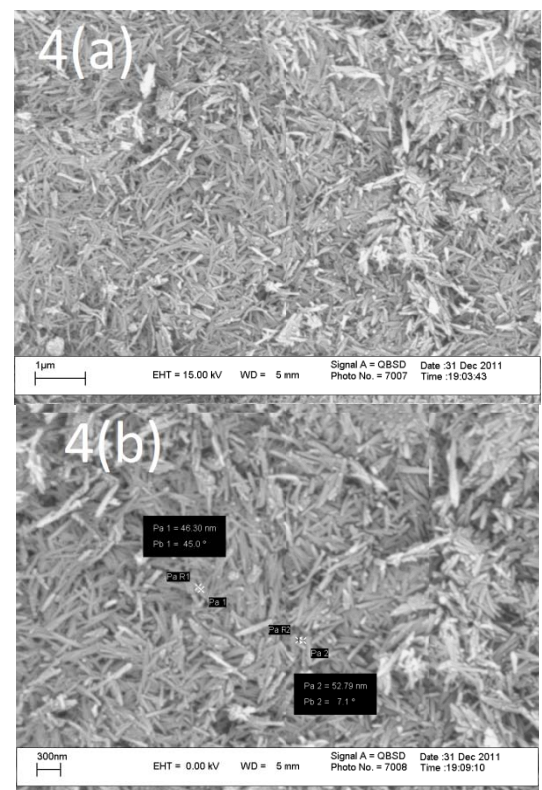


Fig. 4(a) and (b). SEM images of  $\alpha$ -Fe<sub>2</sub>O<sub>3</sub> nanostructures prepared by ultrasound-assisted method at different magnifications.

### 3.3 FT-IR characterization

Fig. 5 shows the FT-IR spectra of FeO(OH) and  $\alpha$ -Fe<sub>2</sub>O<sub>3</sub> nanostructures. As shown in curve a, the Transmission peak at around 3143 cm<sup>-1</sup> related to vibration of  $\alpha$ -FeO(OH)  $\nu$ (O-H), also two sharp peaks at 795 and 890 cm<sup>-1</sup> belonging to torsional vibration modes of  $\delta$ (Fe-O-H) that confirm previous peak. The characteristic transmission peaks at 453 and 647 cm<sup>-1</sup>, which were attributed to the stretching vibration modes of  $\nu$ (Fe-O). After annealing at 450°C, (curve b) three weak peaks around 417, 454 and 505 cm<sup>-1</sup> appear which are assigned to the stretching vibration mode of  $\nu$ (Fe-O) and shows a trend to the phases transition between  $\nu$ (Fe-O) and  $\alpha$ -Fe<sub>2</sub>O<sub>3</sub>. The peaks at 978, 1053 and 1141 cm<sup>-1</sup> related to stretching and torsional vibration mode of sulfate ion. With increasing of temperature up to 450°C (curve b), we see all of the vibration modes of FeO(OH) vanish and other peaks belonging to stretching vibration modes of  $\alpha$ -Fe<sub>2</sub>O<sub>3</sub>. In general the bands of stretching vibration modes of hematite Fe-O are contributed to 360, 385, 485 and 575 cm<sup>-1</sup>.

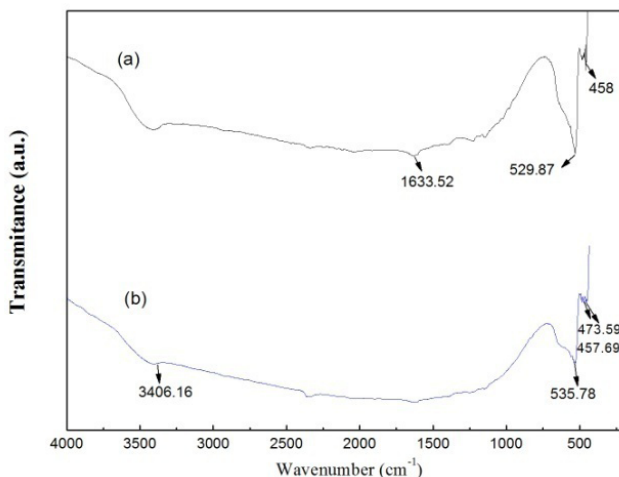


Fig. 5. FT-IR Transmittance spectrum of the prepared samples before thermal annealing (FeO(OH))(a) and after thermal annealing at 450 °C (sample  $\alpha$ -Fe<sub>2</sub>O<sub>3</sub>)(b).

### 4. Conclusion

In conclusion, FeO(OH) and  $\alpha$ -Fe<sub>2</sub>O<sub>3</sub> nanostructures prepared by the facile ultrasound-assisted method from an aqueous FeSO<sub>4</sub>·7H<sub>2</sub>O and NaOH in the presence of 3-MPA as a capping agent and some of structural properties is reported. The XRD structural analysis indicated that the FeO(OH) and  $\alpha$ -Fe<sub>2</sub>O<sub>3</sub> nanostructures were polycrystalline. The SEM images indicated that nanostructures in both cases formed in the polydispersive rod-like shape and the length of nanorods are smaller than 300 nm and the width of nanorods are smaller than 50 nm. The FT-IR transmission spectrum also confirms existence the (Fe-O) and FeO(OH) modes in products.

### Acknowledgement

This work is extracted from a research project at the Islamic Azad University, Takestan Branch. The authors wish to acknowledge the financial support of the vice chancellor in research of Islamic Azad University, Takestan Branch.

### References

- [1] J. A. Rodríguez, M. Fernández-García, (Eds.) Synthesis, Properties and Applications of Oxide Nanoparticles. Wiley: New Jersey, 2007.
- [2] X. U. Peng, Zhuang Hui-Zhao, Optoelectron. Adv. Mater.-Rapid Comm., **5**(12), 1282 (2011).
- [3] J. A. Rodriguez, G. Liu, T. Jirsak, Hrbek, Z. Chang, J. Dvorak, A. Maiti, J. Am. Chem. Soc. **124**, 5247 (2002).
- [4] C. Noguera, Physics and Chemistry at Oxide Surfaces; Cambridge University Press: Cambridge, UK, 1996.
- [5] P. V. Kamat, Chem. Rev. **93**, 267 (1993).
- [6] J. Livage, M. Henry, C. Sanchez, Prog. Solid State Chem. **18**, 259 (1988).
- [7] M. Fernández-García, A. Martínez-Arias, J. C. Hanson, J. A. Rodríguez, Chem. Rev **104**, 4063 (2004).
- [8] R. M. Cornell, U. Schwertmann, The Iron Oxides; Wiley-VCH: Weinheim, Germany, 2003.
- [9] A. I. Anton, J. Magn. Magn. Mater. **85**, 137 (1990).
- [10] R. C. Hollins, Materials for optical limiters, Current Opin. Solid State Mater. Sci. **4**, 189 (1999).
- [11] C. Y. Haw, F. Mohamed, C. H. Chia, S. Radiman, S. Zakaria, N. M. Huang, H. N. Lim, Ceramics International **36**, 1417 (2010).
- [12] M. S. Diallo, N. Savage, Nanoparticles and Water Quality, Journal of Nanoparticle Research, **7**, 325 (2005).
- [13] L. Fu, V. P. Dravid, D. L. Johnson, Appl. Surf. Sci. **181**, 173 (2001).
- [14] R. Bosinceanu, N. Sulitanu, J. Optoelectron. Adv. Mater. **10**(12), 3482 (2008).
- [15] M. Raciciu, D. E. Creangru, Gh. Calugaru, J. Optoelectron. Adv. Mater. **7**(6), 2859 (2005).
- [16] D. Chicea, J. Optoelectron. Adv. Mater. **12**(11), 2208 (2010).
- [17] M. M. Mdleleni, T. Hyeon, K. S. Suslick, J. Am. Chem. Soc. **120**, 6189 (1998).
- [18] Y. Azizian-Kalandaragh, Ali Khodayari, Materials Science in Semiconductor Processing **13**, 225 (2010).
- [19] H. Wang, S. Xu, X. Zhao, J. Zhu, X. Xin, Mater. Sci. Eng. B **96**, 60 (2002).
- [20] Y. Azizian-Kalandaragh, A. Khodayari, Phys. Status Solidi A, **207**(9), 2144 (2010).

- [21] Y. Azizian-Kalandaragh, A. Khodayari, M. Behboudnia, Materials science in semiconductor processing, **12**, 142 (2009).
- [22] T.P. Raming, A.J.A. Winnubst, C.M. Kats, P.A. Philipse, J. Coll. Interface Sci. **249**, 346 (2002).
- [23] Prita, P. Sarangi., Bhanudas Naik, N. N. Ghosh, Powder Technology **192**, 245 (2009).
- [24] J.M., Hwang, M.O., Oh, I., Kim, J.K., Lee, C.S., Ha, Curr. Appl. Phys. **5**, 31 (2005).

---

\*Corresponding author: j.hasanzadeh@tiau.ac.ir,  
j.hasanzadeh@yahoo.com